

DOI: 10.1002/cmdc.200500027

The Potential of P1 Site Alterations in Peptidomimetic Protease Inhibitors as Suggested by Virtual Screening and Explored by the Use of C–C-Coupling Reagents**

Steffen Weik,^[a] Torsten Luksch,^[b] Andreas Evers,^[b] Jark Böttcher,^[b] Christoph A. Sotriffer,^[b] Andrej Hasilik,^[c] Hans-Gerhard Löffler,^[c] Gerhard Klebe,^[b] and Jörg Rademann^{*[a]}

A synthetic concept is presented that allows the construction of peptide isostere libraries through polymer-supported C-acylation reactions. A phosphorane linker reagent is used as a carbanion equivalent; by employing MSNT as a coupling reagent, the C-acylation can be conducted without racemization. Diastereoselective reduction was effected with *L*-selectride. The reagent linker allows the preparation of a norstatine library with full variation of the isosteric positions including the P1 side chain that addresses the protease S1 pocket. Therefore, the concept was employed to investigate the P1 site specificity of peptide isostere inhibitors systematically. The S1 pocket of several aspartic proteases including plasmepsin II and cathepsin D was modeled and docked with

≈ 500 amino acid side chains. Inspired by this virtual screen, a P1 site mutation library was designed, synthesized, and screened against three aspartic proteases (plasmepsin II, HIV protease, and cathepsin D). The potency of norstatine inhibitors was found to depend strongly on the P1 substituent. Large, hydrophobic residues such as biphenyl, 4-bromophenyl, and 4-nitrophenyl enhanced the inhibitory activity (IC_{50}) by up to 70-fold against plasmepsin II. In addition, P1 variation introduced significant selectivity, as up to 9-fold greater activity was found against plasmepsin II relative to human cathepsin D. The active P1 site residues did not fit into the crystal structure; however, molecular dynamics simulation suggested a possible alternative binding mode.

Introduction

Proteases constitute one of the few protein classes widely established as putative drug targets and are involved in pathological states ranging from viral and parasitic infections, through blood pressure, coagulation, and neurodegenerative diseases such as Alzheimer's, to osteoporosis and cancer. Therefore, protease inhibition by small organic compounds has been studied extensively, and protease inhibitors have found broad application as admitted drugs. A plethora of knowledge has been compiled on the design and synthesis of these molecules.^[1–3]

Most reversible protease inhibitors bind to the active site of the enzyme by mimicking the tetrahedral intermediate formed during the catalyzed amide bond cleavage. A noncleavable molecular motif addresses the interaction pattern exposed to the active site; in the considered case of aspartic proteases, peptide isosteres that contain a secondary alcohol or amine have often been used successfully as such 'transition-state mimics'. In these inhibitory structures, the mimicking core addresses the interaction pattern at the catalytic center, notably the interaction with the proteolytic machinery of the enzyme. With its surrogate of the P1 side chain of the natural substrate, it accommodates the S1 binding pocket. Beyond the P1 site, the mimicking core is flanked by extended recognition elements at both ends targeting the binding pockets in either

the N-terminal (S2, S3, S4, ...) or C-terminal direction (S1', S2', S3', ...).

It has been known for a long time that the P1 site is of primordial importance to establish selectivity and affinity in substrate recognition by a particular protease; accordingly many proteases have been categorized with respect to their P1 site

[a] Dr. S. Weik, Prof. Dr. J. Rademann
Leibniz Institute for Molecular Pharmacology (FMP)
Robert-Rössle-Strasse 10, 13125 Berlin (Germany) and
Free University Berlin, Takustrasse 3, 14195 Berlin (Germany)
Fax: (+49) 30-94793280
E-mail: rademann@fmp-berlin.de

[b] T. Luksch, Dr. A. Evers, J. Böttcher, Dr. C. A. Sotriffer, Prof. Dr. G. Klebe
Institute for Pharmaceutical Chemistry
University of Marburg
Marbacher Weg 6, 35032 Marburg (Germany)

[c] Prof. Dr. A. Hasilik, Dr. H.-G. Löffler
Institute for Physiological Chemistry
University of Marburg
Karl-von-Frisch-Strasse 1, 35043 Marburg (Germany)

[**] Essential parts of this work were presented at the 28th European Peptide Symposium in Prague, Czech Republic, September 5–10, 2004, and at Eurocombi 3 in Winchester, England, July 18–22, 2005, where it was assigned a poster award.

Supporting information for this article is available on the WWW under <http://www.chemmedchem.org> or from the author.

specificity. Thus, it can be assumed that also for the molecular skeleton of protease inhibitors, the nature of the P1 site is a determinant for selectivity and affinity. The work presented herein demonstrates a novel, synthesis-based approach to investigate the P1 site contribution in peptidomimetic inhibitors.

In principle, the contribution of individual structural elements to the overall binding affinity of an extended inhibitor structure can be investigated by the systematic variation of the respective elements. This approach assumes that the contributions of the individual elements to the total binding properties are additive. Over the last decade, the systematic variation of side chains within a series of protease inhibitors has been facilitated considerably by the introduction of combinatorial concepts both in solution and on solid phase.^[4–9] However, upon closer inspection, the combinatorial screen has mainly been limited to the flanking regions of the mimicking core. Accordingly, most structure–activity relationship studies of protease inhibitors focus exclusively on the elaborate variation of the C- and N-terminal sites, that is, the P2, P3, ... sites in the N-terminal direction and the P1', P2', ... sites in the C-terminal direction of the native substrate. In contrast, P1 mutations remain largely unexplored and have been studied only in special cases.^[10–13] As a result, elaborate and exhaustive P1 site mutations have not yet been performed to investigate their influence on the affinity or specificity of protease inhibitors. Therefore, we considered the development of novel synthetic strategies leading to efficient P1 mutations as highly attractive goal.

The main reason for limited P1 site variation in peptidomimetics has been the difficult access to diversely substituted isostere building blocks. Classically, peptide isosteres are constructed by multistep synthesis in solution. Often the isosteric core is assembled by a C–C-coupling step that requires harsh conditions as applied for strongly basic carbanion chemistry. For an efficient combinatorial variation of the mimicking core, however, it is necessary to construct an isostere through a C–C-coupling reaction on the polymer support along with the introduction of a side-chain functionality and with simultaneous control of the stereochemistry. For better accessibility, the isosteric cores should be constructed solely from commercially available chiral building blocks such as protected amino acids. All reaction conditions have to be smooth and fully compatible with standard peptide chemistry, thereby excluding the use of harsh reagents such as strong bases, strong acids, etc. To our knowledge, general combinatorial approaches to construct and vary mimicking cores including the P1 substituent purely based on commercially available chiral building blocks (amino acids) using mild reaction conditions have not been reported so far.

Results and Discussion

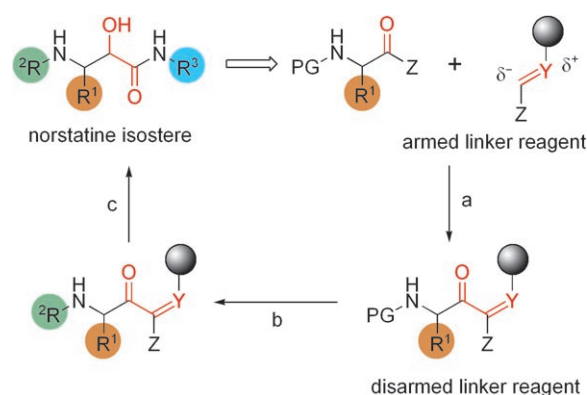
C–C-Coupling reactions are the key step in the synthesis of most peptide isosteres. Therefore, the implementation of such reactions in solid-phase synthesis protocols is a prerequisite for the flexible variation of peptide isosteres. α -Hydroxy- β -amino acids that are found in norstatines, for example, were selected

as a model for the construction of peptide isosteres on solid phase. These isosteres have been reported as efficient inhibitors for several different classes of hydrolases, including aspartic proteases^[4–6,14] and metalloproteases^[15,16] depending on their stereochemistry. Norstatines can be derived directly or indirectly from α -amino aldehydes through the addition of various C1 nucleophiles. Cyanide anions,^[17,18] isocyanide-based multicomponent reactions,^[19–22] and formaldehyde hydrazones^[23,24] have been reported as C nucleophiles in these umpolung reactions; additionally, vinyl Grignard and lithium organic compounds^[25–29] have been used as masked C1 anion equivalents. In these reactions, the stereocontrol in positions 2 and 3 is problematic due to the facile racemization of the amino aldehyde building block and the limited stereospecificity of the nucleophilic attack.

As an alternative, C–C couplings that lead to isosteric building blocks can be furnished by a C-acylation reaction. This strategy mimics the chemistry of the lipid and polyketide pathways in which acylations of thioesters are employed. The C-acylation strategy has a number of distinct advantages over the addition strategy. The preparation of peptide aldehydes is avoided and the chiral pool of amino acids can be used directly. Following the racemization-free acylation of a 1,1-dipole synthon representing a masked carbonyl group, α -keto derivatives are obtained which can be reduced stereospecifically. Thus, the stereochemistry of the norstatine products is controlled separately for both stereocenters.

General approach to norstatine inhibitors

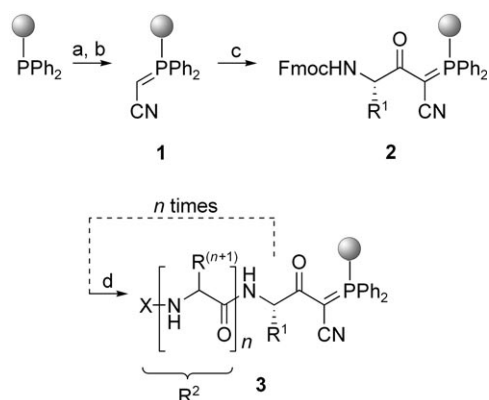
Recently, the solid-phase acylation of phosphoranes was established which represents the first example of the linker reagent concept (Scheme 1).^[30] Therein, in contrast to most applications on polymer supports, the polymer performs a double task: in the first step it acts as an 'armed' polymer reagent, reacting as a stabilized carbanion equivalent in the key C–C coupling. Following the C-acylation reaction, the now 'disarmed' linker reagent serves as a classical linker moiety, that is, a polymeric protecting group that allows multistep solid-phase synthesis without cleaving the linker group. Cleavage of the linker



Scheme 1. Concept of a carbanionic linker reagent in the synthesis of norstatines: a) C–C coupling; b) solid-phase synthesis transformations; c) linker cleavage and modification. Y = masked carbonyl group, Z = leaving group.

reagent finally releases an activated intermediate for further modification.

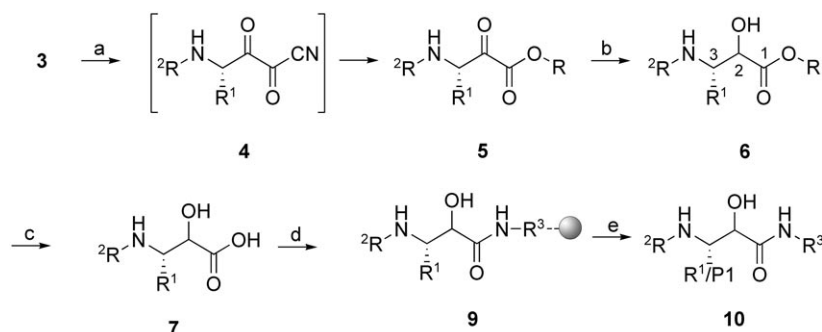
With polymer (cyanomethylene)phosphorane **1** (Scheme 2) as a stabilized ylide and carbanionic armed linker reagent, C-acylations proceeded smoothly to **2** by using EDC and catalytic



Scheme 2. Reagents and conditions: a) BrCH₂CN, toluene, 150 °C, mw, 15 min; b) TEA, CH₂Cl₂, RT, 2 h; c) Fmoc-AA_{R1}-OH, EDC, DMAP (cat.), CH₂Cl₂, RT, 12 h; or d) piperidine/DMF (20:80 v/v), solid-phase peptide synthesis coupling steps with Fmoc-AA_{R2}-OH, DIC, HOBT-H₂O, *n* times, capping (X) after final Fmoc cleavage. DIC = 1,3-disopropylcarbodiimide, DMAP = 4-dimethylaminopyridine, DMF = *N,N*-dimethylformamide, EDC = 3-(3-dimethylamino-propyl)-1-ethylcarbodiimide hydrochloride, Fmoc = 9-fluorenylmethyloxycarbonyl, HOBT = 1-hydroxybenzotriazole, mw = microwave irradiation, TEA = triethylamine.

amounts of 4-dimethylaminopyridine (DMAP) with various Fmoc-protected amino acids while avoiding premature cleavage of the Fmoc group. Following the C–C-coupling step, the chemistry was compatible with Fmoc deprotection and further N-acylations necessary to construct the flanking substituents at the N-terminal side of the isostere **3**.

To construct isostere libraries with variation of the P1 position and the flanking substituents, it was essential to establish the variation of the C-terminal flanking substituents and the stereocontrolled synthesis of the isosteric stereocenters. Oxidative cleavage of the acylated and elongated phosphorane **3** (Scheme 3) appeared to offer direct access to the desired prod-



Scheme 3. Reagents and conditions: a) DMDO/acetone, ROH (R = TMSE, for example), 0 °C, 30 min; b) evaporation, NaBH₄, CH₂Cl₂/EtOH (1:1 v/v), 0 °C, 30 min; c) saponification, for R = TMSE TBAF-3 H₂O or TASF, DMF, RT, 3 h; d) pre-loaded resin **8**, EDC, HOBT-H₂O, DMF, RT, 12 h; e) HFIP/CH₂Cl₂ (20:80 v/v), RT, 3 × 20 min, (TFA/H₂O (95:5 v/v), side chain deprotection if applicable). DMDO = dimethyldioxirane, HFIP = hexafluoroisopropanol, TASF = tris(dimethylamino)sulfonium difluorotrimethylsilicate,^[56] TBAF = tetra-*n*-butylammonium fluoride, TFA = trifluoroacetic acid, TMSE = 2-(trimethylsilyl)ethyl.

uct via an α,β -diketonitrile **4** as a reactive intermediate that could be further converted into hydroxy esters **6** and hydroxy amides (norstatines, **9**) by reaction with alcohols or amines followed by reduction. Ozonolysis of the phosphorane was suggested as the method of choice. Unfortunately, this reaction delivered a decarbonylated by-product. Especially with amines, the formation of this by-product could not be suppressed by variation of the ozonolysis conditions.^[31–33] We found that dimethyldioxirane (DMDO) as oxidant in this reaction yielded the expected α -keto esters exclusively, following the scavenging with alcohols as co-solvents. In contrast, α -keto amides as norstatine precursors required a modified procedure: amines could not be present during cleavage because of their sensitivity to oxidation, and were added only after the removal of excess DMDO. Thus, we decided to follow a reaction pathway via intermediate esters **6**, which were converted into amides **9** by saponification and coupling to the C-terminal building block. Trimethylsilylethyl (TMSE) α -keto esters obtained with trimethylsilylethanol as co-solvent proved to be very suitable intermediates. Following the reduction of keto ester **5**, carboxylic acid **7** was obtained after ester cleavage and was coupled to a second pre-loaded resin carrying the C-terminal substituents for a maximal variation of R³ (species **9**). In a final step, the complete protease inhibitor **10** was cleaved off.

Stereocontrol: racemization-free C-acylation

The stereochemistry of the norstatine building blocks synthesized in the first part of this sequence was initially determined by chiral GC. Complete hydrolysis and derivatization of compound **6** (R¹ = benzyl, R² = Bz-Val, R = TMSE, 2*R* and 2*S*) followed by comparison of the central 3-amino-2-hydroxy-4-phenylbutanoic acids with the corresponding reference compounds revealed the presence of four diastereomers (Figure 1, left). Accordingly, the applied reported acylation conditions led to a racemization of up to 20% in position 3. Therefore, a large number of alternative coupling conditions were studied. 1-(Mesitylene-2-sulfonyl)-3-nitro-1*H*-1,2,4-triazole (MSNT) known from the phosphorylation^[34] and acylation^[35] of hydroxy functions proved to represent the method of choice. The use of MSNT with *N*-methylimidazole as base gave 2.8% racemization. Diisopropylethylamine yielded 0.8% of the racemized diastereomers, whereas racemization could be suppressed completely with 2,6-lutidine as base (Figure 1, right).

Diastereoselective reduction

Diastereomeric mixtures of the final norstatines were obtained by using NaBH₄ for the reduction of intermediate α -keto esters **5**. Therefore, the possibilities for a diastereoselective reduction with conventional re-

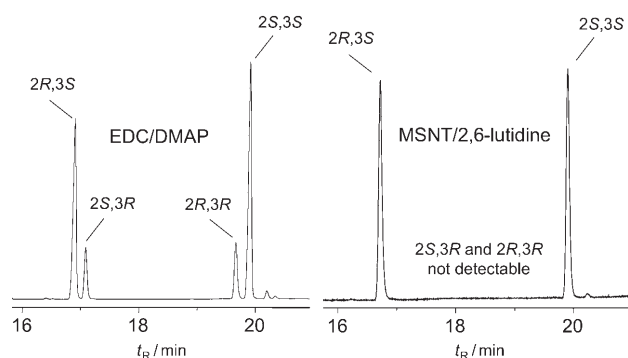


Figure 1. Determination of configurations of the transition-state isomers obtained under different acylation conditions (indicated) by chiral gas chromatography.

agents were scrutinized. Preliminary considerations concerning the favored approach of a hydride equivalent attacking the carbonyl group resulted in the assumption that both Felkin–Anh and chelation-controlled reaction conditions should lead to the same favored product (*syn* = 2*R*,3*S*; Figure 2). Only Lewis-acidic reducing reagents such as DIBAL-H might provide access to the *anti* configuration.

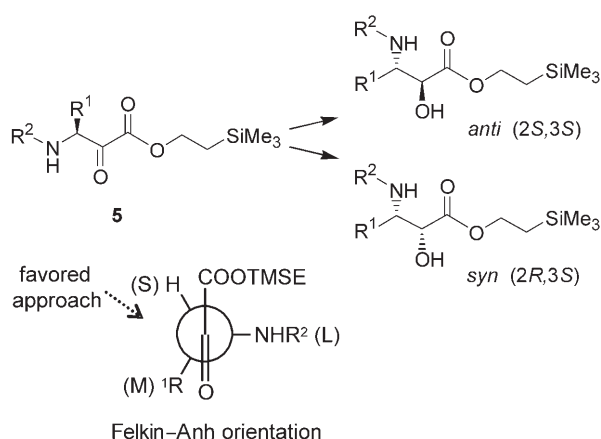


Figure 2. Application of the Felkin–Anh model to the reduction of α -keto TMSE esters **5**. S, M, and L refer to the relative steric bulk (small, medium, and large, respectively) of the groups indicated.

The actual influence of the reducing agents on the product distribution was investigated in the reduction of model compound **5** (R^1 = benzyl, R^2 = Bz-Val, R = TMSE) under various conditions (Table 1). *Syn/anti* ratios were determined by HPLC. As predicted, chelating reagents ($Zn(BH_4)_2$) and others that favor Felkin–Anh products (L-selectride, $LiAlH(OtBu)_3$, $NaBH_4$) showed an accumulation of the *syn* product, whereas DIBAL-H gave a slightly increased amount of the *anti* product. Surprisingly, the high *syn*-selectivity previously reported for the use of $Zn(BH_4)_2$ in the reduction of α -keto amides^[36] was not observed with α -keto ester **5**.^[37] The best results were obtained with L-selectride, which yielded a diastereomeric ratio of 98:2.

Table 1. *Syn/anti* ratios of the reduction products of model compound **5** (R^1 = benzyl, R^2 = Bz-Val, R = TMSE) under various conditions.

Reduction Conditions	d.r. ^[a]
$NaBH_4$, $CH_2Cl_2/EtOH$ (1:1 v/v), 0 °C	48:52
$NaBH_4$, EtOH, –78 °C	33:67
$Zn(BH_4)_2$, THF, –78 °C	40:60
DIBAL-H, THF, –78 °C	56:44
L-Selectride, THF, –95 °C	2:98
$LiAlH(OtBu)_3$, THF, –78 °C	44:56

[a] 2*S*,3*S* (*anti*) : 2*R*,3*S* (*syn*); HPLC at λ = 214 nm.

Virtual screening of the plasmepsin II S1 site and design of a norstatine library

Plasmepsin II, an aspartic protease responsible for the degradation of human hemoglobin in malarial infections, was selected as the first inhibitor target addressed by a P1 mutation library of norstatines. To develop optimally suited P1 occupancy, a virtual screen of putative side-chain decorations for the S1 pocket in plasmepsin II was performed. Starting from the published enzyme–inhibitor complex of plasmepsin II and EH-58 (**11**) containing a hydroxyethylamine isostere (PDB code: 1LF3, Figure 3),^[38] docking studies were carried out by applying the FlexX docking software with a set of potential norstatine inhibitors **10**, which were structurally derived from the published statine inhibitor **12**^[39] (Figure 4). Similar positions and orientations of the P1 residue for the hydroxyethylamine, statine (=hydroxyethyl) and norstatine (=hydroxymethyl) isosteres were obtained. For the purpose of further ligand optimization, the position of the core skeleton was spatially fixed, and the P1 side chain was replaced systematically by 500 amino acid residues referenced in the Sigma–Aldrich and ACD databases. The resulting docking solutions were assessed by a scoring function. Some general conclusions could be derived from these screens: apart from a phenyl residue, which usually addresses S1 in the natural substrate hemoglobin, phenyl moieties substituted by polar residues such as hydroxy or methoxy groups are also predicted to be strong binders (Figure 3b). For an indolyl or substituted indolyl group, hydrogen bonds to a serine side chain in S1 were predicted. Finally, sterically more demanding hydrophobic residues such as naphthyl also received a high score (Figure 3c).

Thus, for synthesis, a small library of 17 norstatine inhibitors solely differing at P1 was assembled based on the indicated preferences found by virtual screening. Some P1 side chains were selected in accordance with the top-scoring virtual screening examples (**10d, e, l, n, o, p**). Further side chains were selected to assess and complement the predictions by spatially and/or electronically modulated hydrophobic side chains not directly suggested in the computational approach. Upon first glance, both configurations of the norstatine building blocks could bind plasmepsin II; accordingly, we decided to synthesize and test controlled mixtures of the corresponding diastereomers.

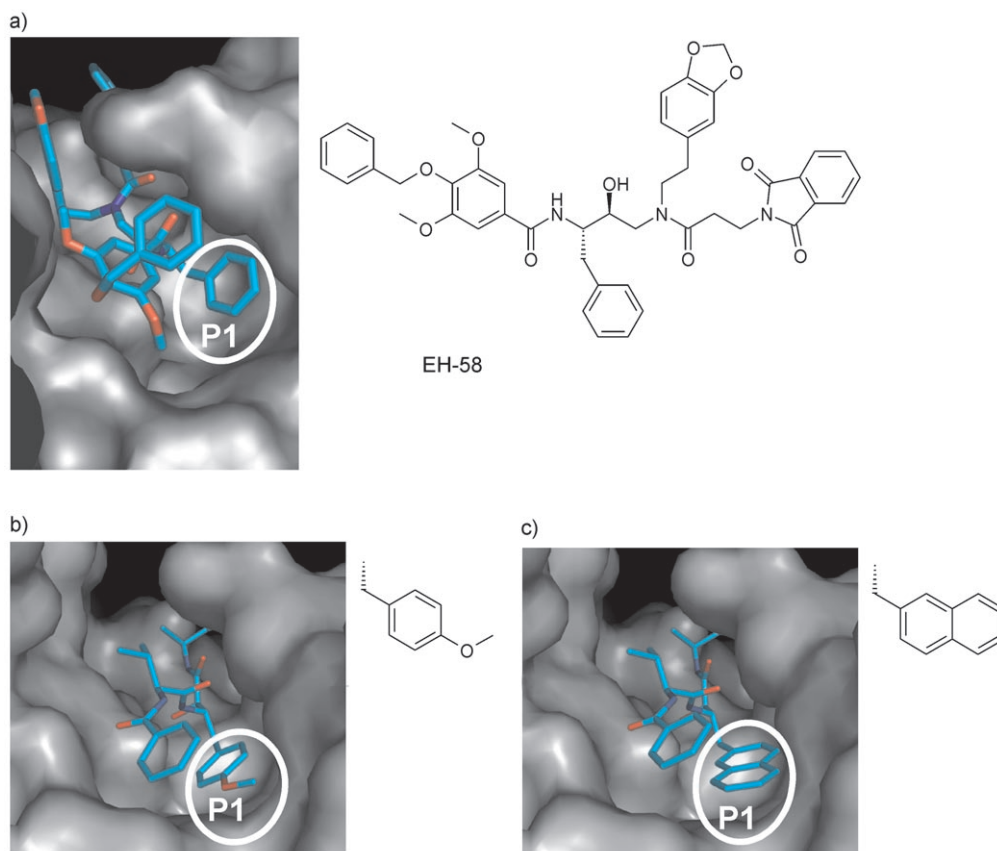


Figure 3. a) Structure and position of inhibitor EH-58 complexed with plasmepsin II.^[38] The phenyl side chain (P1) was systematically exchanged in the designed norstatine analogues by other residues in a docking screen; particularly, b) a 4-methoxy phenyl group and c) a 2-naphthyl moiety were highly scored.

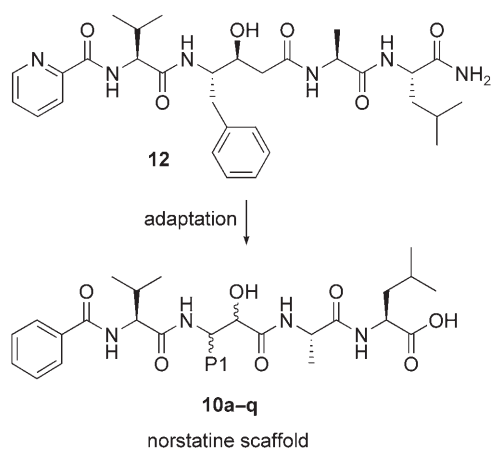


Figure 4. A virtual compound library **10a–q** was designed based on the docking of the norstatines structurally derived from the published statine inhibitor **12**.

Synthesis of the designed norstatine library

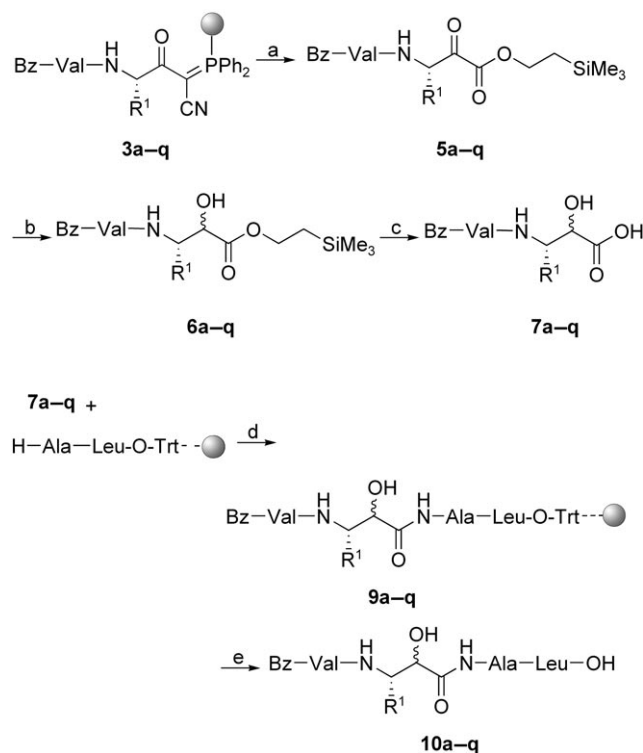
Following the optimized reaction conditions, the synthesis of all designed inhibitors was pursued (Scheme 4). In a first step, various Fmoc-protected amino acids were coupled to cyanomethylene phosphorane resin **1** in yields of 69–88% (**2a–q**). Chain elongation with Fmoc-Leu and benzoyl capping after

Fmoc cleavage led to polymer-bound peptidyl α -keto (cyanomethylene)phosphoranes **3a–q**, which were cleaved by DMDO/TMSE-OH and reduced by NaBH₄ to yield α -hydroxy TMSE esters **6a–q** as diastereomeric mixtures of high purity.^[40] Saponification of esters **6a–q** with TBAF trihydrate (or alternatively with TASF^[56]), immediate activation, and coupling of the free acids **7a–q** to Ala-Leu-TCP resin yielded polymer-supported norstatines **9a–q**, which could be cleaved off in a final step to the desired compounds **10a–q**.

Crude products of high yield and purity (Table 2) were identified by LC–MS and purified by RP HPLC. As explained above, we decided to test mixtures of two diastereomers, and the diastereomeric ratios were determined by ¹H NMR spectroscopy. Signals of each configuration (2S or 2R) could be assigned owing to characteristic chemical shifts of the hydrogen atoms bound to the α -carbon atoms. As a control in the case of **10q**, the resulting diastereomers were separated and assigned as pure compounds.

Screening of inhibitors **10a–q** against plasmepsin II, cathepsin D, and HIV protease

All synthesized compounds **10a–q** were assayed against different aspartic proteases. The main focus was directed toward the inhibition of plasmepsin II and to a comparison with the predicted favorable P1 side chains. Due to its structural similar-



Scheme 4. Reagents and conditions: a) DMDO/acetone, ROH (R = TMSE, for example), 0 °C, 30 min; b) evaporation, NaBH₄, CH₂Cl₂/EtOH (1:1 v/v), 0 °C, 30 min; c) saponification, TASF, DMF, RT, 3 h; d) pre-loaded resin, EDC, HOBT·H₂O, DMF, RT, 12 h; e) HFIP/CH₂Cl₂ (20:80 v/v), RT, 3 × 20 min. Bz = benzoyl, Trt = trityl.

ity with plasmepsin II (35% sequence similarity) human cathepsin D, a lysosomal protease responsible for the degradation of proteins to small peptides, was also considered with particular respect to the selectivity potential of the prepared library. Finally, the inhibition of HIV protease was also determined. Both plasmepsin and HIV protease had been expressed, purified, and activated from the respective pro-enzyme forms as described elsewhere.^[41,42] Cathepsin D was used as the two-chain mature enzyme purified from human placenta.^[43] Compounds **10a–p** were tested as diastereomeric mixtures to allow an overall estimate of their potential.

The lead compound **10a**, which comprises a central phenyl norstatine, was attributed a relative activity of 1; as expected, it displays a lower inhibitory activity (IC₅₀) than that of the natural product pepstatin A. The relative activities of **10b–q** show the contribution of the different P1 side chains to the total inhibition (Table 3). In contrast to the predictions suggested by computer screening, hydrophilic phenyl substituents exhibiting additional hydrogen-bonding potential (in compounds **10o**, **10p**, and **10q**) proved to be less potent as plasmepsin II inhibitors. Similarly, a 1-naphthyl group (in **10d**) or indolyl residue (in **10l**) did not show potent inhibition. However, three norstatines (**10g**, **10j**, and **10k**) with large hydrophobic substituents at the *para* position of the phenyl ring depart significantly in affinity compared with all other members of the series. Clearly, with respect to all three proteases, the biphenyl residue (in **10g**) represents the most potent side chain. Whereas most of the less active compounds showed higher affinity toward cath-

epsin D than toward plasmepsin II, **10g**, **10j**, and **10k** displayed some selectivity in favor of plasmepsin II.

Molecular dynamics simulations indicate adaptability of the S1 pocket

Virtual screening failed to predict ligands with extended P1 residues such as **10g**, **10j**, and **10k** as potent inhibitors for plasmepsin II. Considering the size of the S1 pocket as observed in the crystal structure, it appears to be too confined to accommodate residues of this size. To assess whether this pocket might adapt flexibly to the shape of a bound ligand, molecular dynamics (MD) simulations were performed. As a measure of structural stability, the root mean square deviation (rmsd) from the starting structure as a function of simulation time was calculated based on a superposition of all C α atoms. All rmsd values remained below 1.90 Å, indicating that no significant structural instability was given.

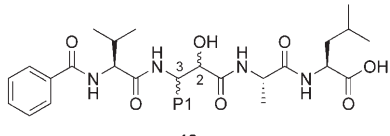
By visual inspection of the simulation trajectory, methionine 15 (M15) was identified as rather flexible amino acid, whereas further residues of the S1 pocket show only minor changes. Quantitative analysis of molecular motion indicates that the χ_1 angle of M15 is not responsible for the large side-chain fluctuation; it only shows standard deviations from average (160°) of $\pm 24^\circ$. In contrast, the χ_2 angle exhibits a high standard deviation of 54° from the mean value of 184°. Besides the conformation found in the crystal structure, two further conformations, in particular, are highly populated and seem to be energetically favorable (Figure 5). Similar observations are made for the χ_3 angle: a high standard deviation of 53° from the average (182°), caused by two highly populated alternative conformations.

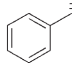
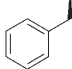
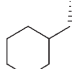
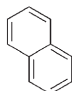
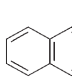
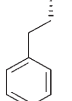
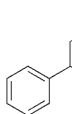
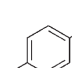
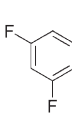
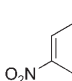
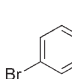
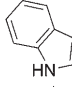

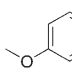
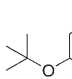
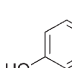
In our initial docking runs, the derivative with the largest P1 side chain was the naphthyl derivative **10d**. For the present analysis, the binding mode of this ligand was extended to a biphenyl substituent. If the conformation of plasmepsin II in the crystal structure (PDB code: 1LF3) is considered, the biphenyl group would be too large and would overlap spatially with the protein (Figure 6a). This explains why we failed to predict such derivatives as promising inhibitor candidates. However, as indicated by the MD simulations, M15 shows pronounced flexibility and can possibly adopt different conformations. In some of the frames collected along the trajectory, a significantly expanded S1 binding pocket is suggested. Taking these protein conformers as a reference, **10g**, **10j**, and **10k** can be accommodated into this site (Figure 6b), thus explaining the enhanced binding affinity of these derivatives with large hydrophobic P1 substituents. This hypothesis is strongly supported by a recently published crystal structure that shows the suggested, conformationally expanded S1 binding pocket in plasmepsin II.^[44]

Conclusions

Herein, we demonstrate the efficacy of the linker reagent concept. By introducing polymer-supported acylations of protected amino acids, a novel and efficient access to norstatine libra-

Table 2. Yields and analytical data for norstatines 10a–q.

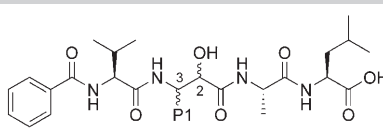
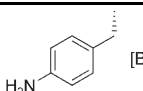


Compd	P1 Side Chain ^[a]	Acylation Yield [%] ^[b]	Purity [%] ^[c]	Isolated Yield [%] ^[d]	d.r. ^[e]
10a		80%	91%	21% (21 mg)	34:66
10b		83%	86%	25% (24 mg)	30:70
10c		71%	87%	27% (23 mg)	48:52
10d		79%	90%	22% (22 mg)	43:57
10e		79%	88%	22% (22 mg)	34:66
10f		79%	90%	26% (25 mg)	51:49
10g		77%	87%	28% (29 mg)	42:58
10h		79%	95%	27% (26 mg)	34:66
10i		74%	87%	18% (17 mg)	30:70
10j		88% ^[f]	84%	20% (22 mg)	40:60
10k		69%	74%	23% (22 mg)	30:70
10l	 [Boc] ^[g]	70%	81%	12 mg	43:57
10m		75%	90%	28% (23 mg)	47:53
10n		79%	94%	25% (24 mg)	35:65
10o		87%	91%	32% (37 mg)	40:60
10p	 [tBu]	87%	90%	22% (22 mg)	67:33

ries has been found. Meanwhile, we have been able to extend the concept to further important isosteric structures.

This synthetic innovation allowed us to scrutinize the relevance of P1 site diversity in a straightforward approach. Virtual screening suggested that P1 site variation, a phenomenon that has been hardly investigated in greater detail until now, might in fact play a prominent role in increasing the affinity and specificity of peptidomimetic inhibitors. FlexX-mediated docking of 500 amino acid side chains was conducted in the active site of the aspartic protease plasmepsin II. Best binding was predicted for inhibitors containing large hydrophobic side chains such as naphthyl groups or large aromatic side chains with additional H-bond donor or acceptor sites. Inspired by the predictions of the virtual screen, a norstatine library was designed to address the S1 site with natural and unnatural amino acid side chains. The synthesis of the norstatine library was carried out by using the linker reagent concept. Norstatine building blocks were constructed on the solid phase through racemization-free C-acylation. Following oxidative cleavage, reduction, and C-terminal elongation on a secondary resin, inhibitor structures were obtained by acidic cleavage from a trityl linker with a purity of $\approx 90\%$ of the crude product.

The norstatines were subjected to inhibition assays against three prominent aspartic proteases: the validated malaria target plasmepsin II, HIV protease, and the homologous human protease cathepsin D. The potency of our norstatine inhibitors was found to depend strongly on the P1 substituent. In the case of plasmepsin II, a large, hydrophobic residue such as biphenyl enhanced the inhibitory activity (IC_{50}) by up to 70-

Table 2. (Continued)					
					
Compd	P1 Side Chain ^[a]	Acylation Yield [%] ^[b]	Purity [%] ^[c]	Isolated Yield [%] ^[d]	d.r. ^[e]
10q	 [Boc] ^[g]	75%	80%	21% (19 mg)	42:58

[a] Initial side chain protecting group indicated in square brackets. [b] Determined by coupling efficiency of first amino acid. [c] Crude product; HPLC at $\lambda=214$ nm. [d] Determined after preparative HPLC. [e] 2*S*,3*S* (*anti*):2*R*,3*S* (*syn*), assigned by ¹H NMR spectroscopy. α -CHOH. [f] *N,N*-diisopropylethylamine (DIPEA) as base instead of 2,6-lutidine. [g] Boc = *tert*-butoxycarbonyl.

Table 3. Inhibitory activity of norstatines 10a–q against plasmepsin II, cathepsin D, and HIV protease.						
Compd	Plasmepsin II		Cathepsin D		HIV Protease	
	IC ₅₀ [μ M]	Rel. Inhib. ^[a]	IC ₅₀ [μ M]	Rel. Inhib. ^[a]	IC ₅₀ [μ M]	Rel. Inhib. ^[a]
10a	346	1	163	1	271	1
10b	> 350	< 1	228	< 1	> 300	< 1
10c	> 350	< 1	25	6.5	285	< 1
10d	300	1.2	34	4.8	ND ^[b]	< 1
10e	110	3.1	32	5.1	100	2.7
10f	> 350	< 1	93	1.8	> 300	< 1
10g	5	69	7	23	14	19
10h	255	1.4	88	1.9	ND ^[b]	< 1
10i	> 350	< 1	43	3.8	100	2.7
10j	25	14	92	1.8	ND ^[b]	< 1
10k	11	32	95	1.7	15	18
10l	> 350	< 1	180	< 1	> 300	< 1
10m	> 350	< 1	> 350	< 1	128	2.1
10n	120	2.9	66	2.5	90	3
10o	> 350	< 1	185	< 1	322	< 1
10p	> 350	< 1	> 350	< 1	583	< 1
10qa (2 <i>S</i> ,3 <i>S</i>)	> 350	< 1	164	1	ND ^[b]	< 1
10qb (2 <i>R</i> ,3 <i>S</i>)	> 350	< 1	93	1.8	ND ^[b]	< 1

[a] Relative inhibition calculated with respect to compound **10a**. [b] Not determined.

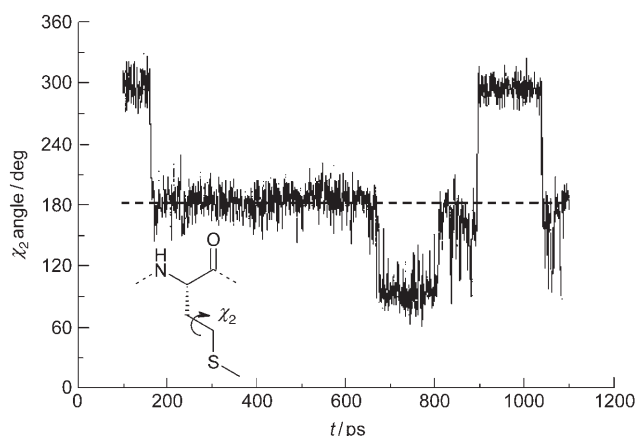


Figure 5. MD simulation (—) of the fluctuation of the χ_2 angle in methionine 15 (M15) of plasmepsin II, with the respective value from the crystal structure (-----) shown as reference; for details, see the Experimental Section.

fold. A similar effect was observed for 4-bromophenyl (30-fold) and 4-nitrophenyl (14-fold). In contrast, hosting additional hydrogen-bond acceptor or donor sites within the S1 pocket did not result in increased inhibitory activity. The enhancing effect was restricted to 4-substituted aromatic residues; both naphthyl and 3,5-disubstituted phenyl groups did not experience significant increase in the inhibitory activity, even though they received high scores in the virtual screen. In addition, P1 variation introduced significant selectivity enhancement: up to 9-fold discrimination advantage was observed for plasmepsin II relative to human cathepsin D. Interestingly, the extended P1 side chain could not be accommodated in the S1 pocket as observed in a crystal structure. However, MD simulations suggest a conformational opening of this pocket which results in a significant increase in the active volume.

In summary, our study indicates the significance of P1 site substitution in peptidomimetic inhibitors against aspartic proteases. This effect has not been recognized so far and might be of considerable value for increasing the affinity and selectivity of protease inhibitors. After completion of our work, two inde-

pendent groups were able to confirm our results impressively. The research groups of Hallberg and Samuelsson reported a 50-fold inhibitory enhancement toward plasmepsin I of a statine (hydroxyethyl) transition-state isostere exhibiting a biphenyl moiety in the opened S1 pocket.^[45] Furthermore, the research group at Actelion Pharmaceuticals communicated a crystal structure exhibiting a biphenyl moiety in the S1 pocket.^[44]

Our results could be realized by a novel synthetic strategy using phosphoranones as linker reagents for C-acylation reactions, thereby allowing a direct incorporation of peptide isostere synthesis in peptide chemistry workflow. Meanwhile, the synthetic concept could be extended to other relevant isosteres which will allow one to scrutinize the effect of P1 variation in further proteases.

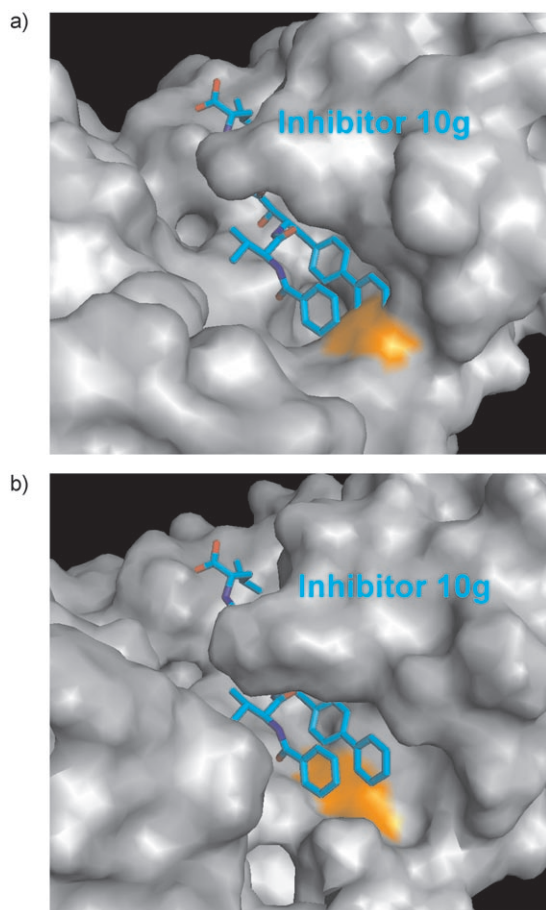


Figure 6. a) Based on the binding mode used in the initial docking study (see Figure 3), the P1 substituent was extended to a biphenyl group as found for the most potent inhibitor **10g**. The protein conformer derived from the crystal structure does not provide sufficient space to accommodate this sterically demanding substituent. b) A modified protein conformer with the M15 side chain (orange surface) populating an alternative conformation as indicated by MD simulation (Figure 5) can favorably host the extended biphenyl ligand.

Experimental Section

General methods: Unless otherwise noted, all reagents were obtained from commercial suppliers and used without further purification. Dry solvents were purchased and stored over molecular sieves. Dimethyldioxirane (DMDO) solution was prepared, dried over molecular sieves (4 Å), and its concentration was calculated from ^1H NMR spectra according to published procedures.^[46,47] Solid-phase chemistry was performed in plastic syringes equipped with Teflon filters. Resins were purchased from Fluka (triphenylphosphine polystyrene) and Pepchem (trityl chloride polystyrene (TCP) resin, Tübingen, Germany). Microwave-assisted solid-phase reactions were performed on a Personal Chemistry SmithSynthesizer. Resins were washed with MeOH, DMF, THF, and CH_2Cl_2 unless otherwise stated. Resin loadings were determined by elemental analysis and photometric determination after Fmoc cleavage. Solid-phase reactions were monitored through FT-ATR-IR spectra of the resins with a Bruker Vector 22/Harrick SplitPea ATR unit. Absorptions are reported in wavenumbers (cm^{-1}). Analysis of cleaved intermediates and products was performed on an analytical HPLC column (5 μm , 250×2 mm, Nucleosil 100 RP-C18) with detection at $\lambda = 214$ nm. Eluents A (0.1% TFA in water) and B (0.1% TFA in ace-

tonitrile) were used in a linear gradient (10% B \rightarrow 100% B in 45 min). Compounds were purified on a semipreparative HPLC column (10 μm , 250×20 mm, Grom-SIL 300 ODS-5 ST RP-C18) employing individual gradients derived from analytical runs (eluent A and B). ESIMS was recorded on an Esquire 3000plus (Bruker). Chiral GC-EIMS was performed on a HP 6890 series GC system coupled to the mass-selective detector (HP 5973) with helium as carrier gas equipped with a Chirasil-Val capillary column. ^1H and ^{13}C NMR spectroscopy were conducted on a Bruker AVANCE 400 instrument. All spectra were obtained in $[\text{D}_6]\text{DMSO}$, and chemical shifts are recorded in ppm (δ) relative to the internal solvent peak ($\delta = 2.50$ ppm for ^1H and $\delta = 39.52$ ppm for ^{13}C). Coupling constants (J) are reported in Hz.

(Cyanomethylene)triphenylphosphorane resin 1: Triphenylphosphine polystyrene (0.5 g, 1.6 mmol g^{-1} , 0.8 mmol, 1% divinyl benzene, 100–200 mesh) was weighed into a microwave vial and suspended in dry toluene (4 mL). After the addition of bromoacetonitrile (266 μL , 4 mmol, 5 equiv) the vial was sealed and heated at 150°C for 15 min in a microwave oven. The vial was cooled to room temperature before opening, and the resin was filtered and washed with dry toluene, CH_2Cl_2 , and ether. The obtained polymer phosphonium salt was resuspended in dry CH_2Cl_2 (5 mL), and TEA (558 μL , 4 mmol, 5 equiv) was added. After shaking for 2 h at room temperature, the orange-colored resin was filtered, washed, and dried in vacuo. IR (ATR): $\tilde{\nu} = 3056, 3025, 2926, 2854, 2149, 1750, 1599, 1492, 1452, 1437, 1256, 1185, 1107, 851, 748, 697, 569, 540, 508 \text{ cm}^{-1}$.

General acylation procedure for coupling (cyanomethylene)triphenylphosphorane resin 1 and Fmoc-amino acids to generate acyl(cyanomethylene)triphenylphosphorane resins 2a–q: (Cyanomethylene)triphenylphosphorane resin 1 (200 mg, 1.51 mmol g^{-1} , 0.302 mmol) was pre-swollen in dry CH_2Cl_2 . The respective Fmoc-amino acid (0.755 mmol, 2.5 equiv) was suspended in dry CH_2Cl_2 (4 mL) and dissolved by the addition of 2,6-lutidine (84 μL , 0.725 mmol, 2.4 equiv). The clear solution obtained after the addition of MSNT (224 mg, 0.755 mmol, 2.5 equiv) was directly mixed with the resin suspension and shaken for 45 min at room temperature. After filtration and rinsing with dry CH_2Cl_2 , the procedure was repeated once. The resin was washed after the double coupling step and dried in vacuo. Acylation yields were determined after Fmoc cleavage of small samples. (Note: DIPEA (124 μL , 0.725 mmol, 2.4 equiv) was used as base in the coupling of Fmoc-4-nitrophenylalanine due to better solubility.) Example IR (ATR, Fmoc-phenylalanine): $\tilde{\nu} = 3404, 3058, 3025, 2921, 2852, 2175, 1719, 1591, 1493, 1451, 1438, 1355, 1241, 1178, 1108, 1030, 756, 740, 698, 538, 505 \text{ cm}^{-1}$.

Peptide elongation and capping of acyl(cyanomethylene)triphenylphosphorane resins 2a–q to peptidyl- α -keto(cyanomethylene)triphenylphosphorane resins 3a–q: Fmoc protecting groups were cleaved with piperidine/DMF (20:80 v/v, 2×6 min). The deprotected resin (0.302 mmol) was washed and suspended in dry DMF. Fmoc-Val-OH (512 mg, 1.51 mmol, 5 equiv) and HOBt- H_2O (184 mg, 1.51 mmol, 5 equiv) were dissolved in dry DMF (4 mL), pre-activated by the addition of DIC (234 μL , 1.51 mmol, 5 equiv), and added to the resin following standard Fmoc solid-phase peptide synthesis. The mixture was shaken for 3 h at room temperature, filtered, and the resin was washed. The procedure (cleavage and coupling step) was repeated with benzoic acid (184 mg, 1.51 mmol, 5 equiv) for benzoyl capping.

Oxidative cleavage of peptidyl- α -keto(cyanomethylene)triphenylphosphorane resins 3a–q to peptidyl- α -ketotrimethylsilyleth-

yl esters 5a–q: Peptidyl- α -keto(cyanomethylene)triphenylphosphorane resins **3a–q** (initially 0.302 mmol) were pre-swollen in minimal dry CH_2Cl_2 in 50-mL round-bottom flasks. Trimethylsilylethanol (30 equiv) was added and the suspensions were stirred carefully (the exact absolute amount of alcohol added differed and referred to the extent of acylation determined after the initial coupling step). Freshly prepared cool DMDO solutions (12 mL each, $\approx 0.072 \text{ mmol mL}^{-1}$, 0.864 mmol, 3–4 equiv, -20°C) were added, and the mixtures were stirred for 30 min at 0°C in which the orange-colored resins grew pale (note: cleavage from resin **31** was carried out by the use of only an equimolar amount of DMDO (2 equiv) slowly added with a syringe pump over the course of 30 min while stirring). DMDO, acetone, and CH_2Cl_2 were removed in vacuo with only gentle warming of the flasks to concentrate the cleavage products in trimethylsilylethanol. After the addition of CH_2Cl_2 (4 mL) the resins were filtered and washed with further CH_2Cl_2 (4 mL) and EtOH ($2 \times 4 \text{ mL}$). The cleavage products dissolved in the combined filtrates, and washings were directly carried on to the next step (reduction, see below) to prevent any potential epimerization.

Reduction of peptidyl- α -ketotrimethylsilylethyl esters 5a–q to peptidyl- α -hydroxytrimethylsilylethyl esters 6a–q: Cleavage products **5a–q** dissolved in $\text{CH}_2\text{Cl}_2/\text{EtOH}$ (1:1 v/v) and trimethylsilylethanol (see above) were cooled to 0°C . NaBH_4 (0.625 equiv, 2.5 equiv in hydride) was dissolved in EtOH (0.5 mL), the solutions were added, and the mixtures were stirred for 30 min at 0°C (the exact absolute amount of NaBH_4 differed in each reaction according to different amounts of substance assuming a cleavage yield of 80%). The clear solutions were allowed to warm to room temperature and were filtered through short plugs of silica gel to remove any inorganic salts. Solvents were removed in vacuo by applying an oil pump. Reaction products were lyophilized from *tert*-butyl alcohol/water (4:1 v/v). The white solids obtained were characterized by HPLC and LC–MS and were directly carried on to the next step without purification (note: only compounds **6l** were purified by preparative HPLC because of lower purity). As an example, diastereomers **6aa** and **6ab** were separated by preparative HPLC and the configuration of the α -hydroxy- β -amino motif was assigned by using chiral GC–MS and reference compounds (after total hydrolysis and derivatization). A representative selection of further diastereomeric mixtures (**10c**, **10i**, and **10n**) was investigated in the same way.

N-(Bz-Val)-2-(trimethylsilyl)ethyl-(2S,3S)-3-amino-2-hydroxy-4-phenylbutanoate (6aa): $^1\text{H NMR}$ (400.16 MHz, $[\text{D}_6]\text{DMSO}$): $\delta = 8.09$ (d, $^3J = 9.09 \text{ Hz}$, 1H, NH_i), 7.89 (d, $^3J = 8.84$, 1H, NH_i), 7.84 (d, $^3J = 7.58 \text{ Hz}$, 2H, arom. CH), 7.46–7.56 (m, 3H, arom. CH), 7.05–7.17 (m, 5H, arom. CH), 5.81 (d, $^3J = 6.06 \text{ Hz}$, 1H, $\text{C}^\alpha\text{HOH}$), 4.28–4.37 (m, 1H, C^βH), 4.23 (dd, $^3J = 8.59 \text{ Hz}$, 8.59 Hz, 1H, $\text{C}^\alpha\text{H Val}$), 3.96–4.04 (m, 1H, $\text{C}^\alpha\text{HOH}$), 3.92–4.13 (m, 2H, OCH_2), 2.64–2.80 (m, 2H, $\text{C}^\gamma\text{H}_2$), 1.92–2.02 (m, 1H, $\text{C}^\beta\text{H Val}$), 0.87–0.98 (m, 2H, SiCH_2), 0.81 (d, $^3J = 6.57 \text{ Hz}$, 3H, $\text{CH}_3 \text{ Val}$), 0.72 (d, $^3J = 6.57 \text{ Hz}$, 3H, $\text{CH}_3 \text{ Val}$), 0.01 ppm (s, 9H, $\text{Si}(\text{CH}_3)_3$); $^{13}\text{C NMR}$ (100.62 MHz, $[\text{D}_6]\text{DMSO}$): $\delta = 172.22$ (C4), 170.41 (C12), 166.20 (C17), 138.45 (C8), 134.41 (C18), 131.26 (C21), 129.20 (C9), 128.23 (C10), 127.92 (C19), 127.48 (C20), 125.93 (C11), 72.43 (C5), 62.34 (C3), 59.11 (C13), 52.67 (C6), 35.01 (C7), 30.20 (C14), 19.29, 18.69 (C15, C16), 16.86 (C2), -1.52 ppm (C1); ESIMS m/z ($M(\text{TMSE ester})$): calcd for $\text{C}_{27}\text{H}_{38}\text{N}_2\text{O}_5\text{Si}$: 498.25, found: 521.3 $[M+\text{Na}]^+$.

N-(Bz-Val)-2-(trimethylsilyl)ethyl-(2R,3S)-3-amino-2-hydroxy-4-phenylbutanoate (6ab): $^1\text{H NMR}$ (400.16 MHz, $[\text{D}_6]\text{DMSO}$): $\delta = 8.16$ (d, $^3J = 8.59 \text{ Hz}$, 1H, NH_i), 7.86 (d, $^3J = 7.33 \text{ Hz}$, 2H, arom. CH), 7.76 (d, $^3J = 9.35 \text{ Hz}$, 1H, NH_i), 7.44–7.57 (m, 3H, arom. CH), 7.09–7.23

(m, 5H, arom. CH), 5.62 (d, $^3J = 6.06 \text{ Hz}$, 1H, $\text{C}^\alpha\text{HOH}$), 4.30–4.38 (m, 1H, C^βH), 4.25 (dd, $^3J = 8.34 \text{ Hz}$, 8.34 Hz, 1H, $\text{C}^\alpha\text{H Val}$), 3.97–4.04 (m, 1H, $\text{C}^\alpha\text{HOH}$), 3.99–4.09 (m, 2H, OCH_2), 2.64–2.89 (m, 2H, $\text{C}^\gamma\text{H}_2$), 1.99–2.09 (m, 1H, $\text{C}^\beta\text{H Val}$), 0.85–0.95 (m, 2H, SiCH_2), 0.84 (d, $^3J = 6.56 \text{ Hz}$, 3H, $\text{CH}_3 \text{ Val}$), 0.79 (d, $^3J = 6.56 \text{ Hz}$, 3H, $\text{CH}_3 \text{ Val}$), -0.03 ppm (s, 9H, $\text{Si}(\text{CH}_3)_3$); $^{13}\text{C NMR}$ (100.62 MHz, $[\text{D}_6]\text{DMSO}$): $\delta = 172.29$ (C4), 170.43 (C12), 166.33 (C17), 138.38 (C8), 134.42 (C18), 131.24 (C21), 129.11 (C9), 128.20 (C10, C19), 127.50 (C20), 126.15 (C11), 70.36 (C5), 62.32 (C3), 59.03 (C13), 53.08 (C6), 37.08 (C7), 29.87 (C14), 19.34, 18.54 (C15, C16), 16.77 (C2), -1.55 (C1); ESIMS m/z ($M(\text{TMSE ester})$): calcd for $\text{C}_{27}\text{H}_{38}\text{N}_2\text{O}_5\text{Si}$: 498.25, found: 521.3 $[M+\text{Na}]^+$.

Determination of configuration of the isosteric motif of compounds 6aa and 6ab by chiral GC–MS: Peptidyl- α -hydroxytrimethylsilylethyl esters **6a** were hydrolyzed in a sealed vial (6N HCl, 110°C , 24 h), the components were derivatized to ethyl esters (2N HCl/EtOH, 110°C , 30 min), and the amino and hydroxy functions were trifluoroacetylated (TFAA/ CH_2Cl_2 , room temperature, 30 min). Fmoc protecting groups of used reference compounds (3-amino-2-hydroxy-4-phenylbutanoic acids) were cleaved with piperidine/ CH_2Cl_2 and treated in the same way. Analytical runs were conducted on a Chirasil-Val capillary column (80°C for 2 min (isotherm.) then 4°C min^{-1} to 190°C). Configurations of isosteres of **6a** were assigned by comparison with the references.

Diastereoselective reduction of peptidyl- α -ketotrimethylsilylethyl esters 5: As an example, the diastereoselective reduction of keto ester **5a** was investigated. Ester **5a** (10 mg, 0.02 mmol) was weighed into a Schlenk tube equipped with magnetic stirrer, screw-cap, and septum, dissolved in the respective dry solvent (2 mL) and cooled.

Variation 1: NaBH_4 (0.5 mg, 0.0125 mmol, 0.625 equiv) was added to the starting material dissolved in EtOH, and the mixture was stirred 2 h at -78°C .

Variation 2: A solution of $\text{Zn}(\text{BH}_4)_2$ in THF prepared according to published procedures^[48] ($18.2 \mu\text{L}$, $0.55 \text{ mmol mL}^{-1}$, 0.01 mmol, 0.5 equiv) was added to the starting material dissolved in dry THF, and the mixture was stirred 2 h at -78°C .

Variation 3: A solution of DIBAL-H in THF ($120 \mu\text{L}$, 1 mmol mL^{-1} , 0.12 mmol, 6 equiv) was added to the starting material dissolved in dry THF, and the mixture was stirred 2 h at -78°C .

Variation 4: A solution of L-selectride in THF ($60 \mu\text{L}$, 1 mmol mL^{-1} , 0.06 mmol, 3 equiv) was added to the starting material dissolved in dry THF, and the mixture was stirred 2 h at -95°C .

Variation 5: $\text{LiAlH}(\text{OtBu})_3$ (7.6 mg, 0.03 mmol, 1.5 equiv) was added to the starting material dissolved in dry THF, and the mixture was stirred 2 h at -78°C .

Work-up for variation 1: The mixture was diluted with MeOH (4 mL), allowed to warm to room temperature, and stirred for 1 h. The solution was filtered over a short plug of silica gel, and the solvent was removed in vacuo.

Work-up for variations 2–5: The reaction was quenched with a solution of citric acid (10% m/m, 2 mL) and extracted with EtOAc ($2 \times 5 \text{ mL}$). The combined organic phase was washed with water and brine (5 mL each), dried over MgSO_4 , and filtered over a short plug of silica gel. The solvent was removed in vacuo.

Syn/anti ratios were determined by analytical HPLC of the crude reaction products.

Loading and solid-phase peptide synthesis on TCP resin; synthesis of Fmoc-Ala-Leu-TCP resin. Dry TCP resin (1 g, 1.5 mmol g^{-1} , 1.5 mmol) was weighed into a plastic filter column. Fmoc-Leu-OH (531 mg, 1.5 mmol, 1 equiv) was dissolved in dry CH_2Cl_2 (10 mL) under the addition of DIPEA ($770 \mu\text{L}$, 4.5 mmol, 3 equiv) and the solution was directly added to the resin. Further CH_2Cl_2 was added

to allow an effective shaking of the mixture. After 1 h at room temperature, dry MeOH (3 mL) was added to cap any remaining trityl chloride functions, and the mixture was shaken for another 15 min, after which the resin was filtered and washed. Quantitative Fmoc determination revealed a loading of 0.81 mmol g^{-1} (80%). Fmoc protecting groups were cleaved with piperidine/DMF (20:80 v/v, $2 \times 6 \text{ min}$). The deprotected resin (1.2 mmol) was washed and suspended in dry DMF. Fmoc-Ala-OH (1.98 g, 6 mmol, 5 equiv) and HOBt-H₂O (919 mg, 6 mmol, 5 equiv) were dissolved in dry DMF (15 mL), pre-activated by the addition of DIC (930 μL , 6 mmol, 5 equiv), and added to the resin following standard Fmoc solid-phase peptide synthesis. The mixture was shaken for 3 h at room temperature, filtered, and the resin was washed and dried in vacuo. The Fmoc-Ala-Leu-TCP resin obtained had a loading of 0.78 mmol g^{-1} .

Saponification of peptidyl- α -hydroxytrimethylsilylethyl esters 6a–q to peptidyl- α -hydroxy acids 7a–q: Peptidyl- α -hydroxytrimethylsilylethyl esters 6a–q (0.119–0.187 mmol) were dissolved in dry DMF (2 mL). TBAF trihydrate (3 equiv) was added, and the clear solution was stirred for 2 h at room temperature. HPLC revealed the total disappearance of starting material (note: TBAF trihydrate can be replaced with an equal amount of TASF, a mild non-alkaline deprotection reagent for silyl protecting groups^[56]). The solutions of the free acids were directly used for the next step without isolation or purification (see below).

Coupling of peptidyl- α -hydroxy acids 7a–q to Ala-Leu-TCP resin and cleavage of norstatines 10a–q: Free peptidyl- α -hydroxy acids 7a–q (0.119–0.187 mmol) dissolved in dry DMF (in the presence of TBAF trihydrate or TASF, see above) were pre-activated through the addition of EDC (0.143–0.224 mmol, 1.2 equiv) and HOBt-H₂O (0.143–0.224 mmol, 1.2 equiv) to the solutions. Fmoc-Ala-Leu TCP resin (0.78 mmol g^{-1} , 0.080–0.125 mmol, 0.67 equiv) was weighed into plastic syringes equipped with filters, deprotected with piperidine/DMF (20:80 v/v, $2 \times 6 \text{ min}$), washed, and suspended in dry DMF. The prepared solutions of pre-activated peptidyl α -hydroxy acids were added and shaken for 12 h at room temperature. Afterward, the resins were filtered and washed. Norstatines 10a–q were cleaved off the resins by treatment with HFIP/CH₂Cl₂ (20:80 v/v, $3 \times 20 \text{ min}$), combination of the solutions, and removal of the solvents in vacuo. Products bearing additional acid-sensitive protecting groups were treated with TFA/water (95:5 v/v, $2 \times 1 \text{ h}$). The crude norstatines were lyophilized from *tert*-butyl alcohol/water (4:1 v/v) and purified by preparative HPLC. Only diastereomers 10qa and 10qb could be separated. All products were characterized by HPLC, LC-ESIMS, ESIMS, and NMR spectroscopy.

N-[N-(Bz-Val)-(2RS,3S)-3-amino-2-hydroxy-4-phenylbutanoyl]-Ala-Leu-OH 10a: ESIMS *m/z* (*M*(norstatine)): calcd for C₃₁H₄₂N₄O₇: 582.31, found: 605.5 [*M*+Na]⁺.

N-[N-(Bz-Val)-(2RS,3R)-3-amino-2-hydroxy-4-phenylbutanoyl]-Ala-Leu-OH 10b: ESIMS *m/z* (*M*(norstatine)): calcd for C₃₁H₄₂N₄O₇: 582.31, found: 605.4 [*M*+Na]⁺.

N-[N-(Bz-Val)-(2RS,3S)-3-amino-4-cyclohexyl-2-hydroxybutanoyl]-Ala-Leu-OH 10c: ESIMS *m/z* (*M*(norstatine)): calcd for C₃₁H₄₈N₄O₇: 588.35, found: 611.5 [*M*+Na]⁺.

N-[N-(Bz-Val)-(2RS,3S)-3-amino-2-hydroxy-4-(1-naphthyl)butanoyl]-Ala-Leu-OH 10d: ESIMS *m/z* (*M*(norstatine)): calcd for C₃₅H₄₄N₄O₇: 632.32, found: 655.4 [*M*+Na]⁺.

N-[N-(Bz-Val)-(2RS,3S)-3-amino-2-hydroxy-4-(2-naphthyl)butanoyl]-Ala-Leu-OH 10e: ESIMS *m/z* (*M*(norstatine)): calcd for C₃₅H₄₄N₄O₇: 632.32, found: 655.5 [*M*+Na]⁺.

N-[N-(Bz-Val)-(2RS,3S)-3-amino-5-phenyl-2-hydroxypentanoyl]-Ala-Leu-OH 10f: ESIMS *m/z* (*M*(norstatine)): calcd for C₃₂H₄₄N₄O₇: 596.32, found: 619.4 [*M*+Na]⁺.

N-[N-(Bz-Val)-(2RS,3S)-3-amino-4-(1,1'-biphenyl-4-yl)-2-hydroxybutanoyl]-Ala-Leu-OH 10g: ESIMS *m/z* (*M*(norstatine)): calcd for C₃₇H₄₆N₄O₇: 658.34, found: 681.3 [*M*+Na]⁺.

N-[N-(Bz-Val)-(2RS,3S)-3-amino-2-hydroxy-4-(4-methylphenyl)butanoyl]-Ala-Leu-OH 10h: ESIMS *m/z* (*M*(norstatine)): calcd for C₃₂H₄₄N₄O₇: 596.32, found: 619.4 [*M*+Na]⁺.

N-[N-(Bz-Val)-(2RS,3S)-3-amino-4-(3,5-difluorophenyl)-2-hydroxybutanoyl]-Ala-Leu-OH 10i: ESIMS *m/z* (*M*(norstatine)): calcd for C₃₁H₄₀F₂N₄O₇: 618.29, found: 641.4 [*M*+Na]⁺.

N-[N-(Bz-Val)-(2RS,3S)-3-amino-2-hydroxy-4-(4-nitrophenyl)butanoyl]-Ala-Leu-OH 10j: ESIMS *m/z* (*M*(norstatine)): calcd for C₃₁H₄₁N₅O₇: 627.29, found 650.3 [*M*+Na]⁺.

N-[N-(Bz-Val)-(2RS,3S)-3-amino-4-(4-bromophenyl)-2-hydroxybutanoyl]-Ala-Leu-OH 10k: ESIMS *m/z* (*M*(norstatine)): calcd for C₃₁H₄₁BrN₄O₇: 660.22/662.22, found 683.4/685.2 [*M*+Na]⁺.

N-[N-(Bz-Val)-(2RS,3S)-3-amino-2-hydroxy-4-(1*H*-indol-3-yl)butanoyl]-Ala-Leu-OH 10l: ESIMS *m/z* (*M*(norstatine)): calcd for C₃₃H₄₃N₅O₇: 621.32, found 644.4 [*M*+Na]⁺.

N-[N-(Bz-Val)-(2RS,3S)-3-amino-4-cyclopropyl-2-hydroxybutanoyl]-Ala-Leu-OH 10m: ESIMS *m/z* (*M*(norstatine)): calcd for C₂₈H₄₂N₄O₇: 546.31, found 569.4 [*M*+Na]⁺.

N-[N-(Bz-Val)-(2RS,3S)-3-amino-2-hydroxy-4-(4-methoxyphenyl)butanoyl]-Ala-Leu-OH 10n: ESIMS *m/z* (*M*(norstatine)): calcd for C₃₂H₄₄N₄O₈: 612.32, found 635.4 [*M*+Na]⁺.

N-[N-(Bz-Val)-(2RS,3S)-3-amino-4-(4-*tert*-butoxyphenyl)-2-hydroxybutanoyl]-Ala-Leu-OH 10o: ESIMS *m/z* (*M*(norstatine)): calcd for C₃₅H₅₀N₄O₈: 654.36, found 677.5 [*M*+Na]⁺.

N-[N-(Bz-Val)-(2RS,3S)-3-amino-2-hydroxy-4-(4-hydroxyphenyl)butanoyl]-Ala-Leu-OH 10p: ESIMS *m/z* (*M*(norstatine)): calcd for C₃₁H₄₂N₄O₈: 598.30, found 621.4 [*M*+Na]⁺.

N-[N-(Bz-Val)-(2S,3S)-3-amino-4-(4-aminophenyl)-2-hydroxybutanoyl]-Ala-Leu-OH 10qa: ¹H NMR (400.16 MHz, [D₆]DMSO): δ = 8.30 (d, ³*J* = 7.83 Hz, 1H, NH_I), 8.14 (d, ³*J* = 9.09 Hz, 1H, NH_I), 7.81–7.91 (m, 3H, arom. CH C25, NH_I), 7.78 (d, ³*J* = 7.33 Hz, 1H, NH_{II}), 7.45–7.58 (m, 3H, arom. CH C26, C27), 7.09 (d, ³*J* = 8.34 Hz, 2H, arom. CH C15), 6.85 (d, ³*J* = 8.09 Hz, 2H, arom. CH C16), 6.07 (bs, 1H, C^αHOH), 4.30–4.43 (m, 2H, C^αH Ala C8, C^βH C12), 4.15–4.29 (m, 2H, C^αH Leu C2, C^αH Val C19), 3.93 (bs, 1H, C^αHOH C11), 2.27–2.49 (m, 2H, C^γH₂ C13), 1.97–2.08 (m, 1H, C^βH Val C20), 1.58–1.69 (m, 1H, C^γH Leu C4), 1.47–1.57 (m, 2H, C^βH₂ Leu C3), 1.23 (d, ³*J* = 6.82 Hz, 3H, CH₃ Ala C9), 0.89 (d, ³*J* = 6.57 Hz, 3H, CH₃ Leu C5, C6), 0.80–0.86 (m, 6H, CH₃ Leu C5, C6, CH₃ Val C21, C22), 0.75 ppm (d, ³*J* = 6.57 Hz, 3H, CH₃ Val C21, C22); ¹³C NMR (100.62 MHz, [D₆]DMSO): δ = 173.84 (C1), 171.89 (C7), 170.85 (C10), 170.46 (C20), 166.41 (C25), 134.50, 131.27, 130.01, 128.27, 127.50, 119.27 (C14–C17, C24–C27), 73.25 (C11), 59.09 (C19), 52.98 (C12), 50.18 (C2), 47.38 (C8), 39.34 (C3), 33.51 (C13), 30.27 (C20), 24.27 (C4), 22.88, 21.26 (C5, C6), 19.42, 18.64 (C21, C22), 19.05 ppm (C9); ESIMS *m/z* (*M*(norstatine)): calcd for C₃₁H₄₃N₅O₇: 597.32, found 598.4 [*M*+H]⁺.

N-[N-(Bz-Val)-(2R,3S)-3-amino-4-(4-aminophenyl)-2-hydroxybutanoyl]-Ala-Leu-OH 10qb: ¹H NMR (400.16 MHz, [D₆]DMSO): δ = 8.31 (d, ³*J* = 7.83 Hz, 1H, NH_I), 8.03 (d, ³*J* = 8.59 Hz, 1H, NH_I), 7.84 (d, ³*J* = 7.33 Hz, 2H, arom. CH C25), 7.80 (d, ³*J* = 7.08 Hz, 1H, NH_{II}), 7.71 (d, ³*J* = 9.09 Hz, 1H, NH_{II}), 7.43–7.56 (m, 3H, arom. CH C26,

C27), 7.24 (d, $^3J=8.34$ Hz, 2H, arom. CH C15), 7.04 (d, $^3J=8.34$ Hz, 2H, arom. CH C16), 6.18 (bs, 1H, C^αHOH), 4.17–4.36 (m, 4H, C^αH Ala C8, C^βH C12, C^αH Leu C2, C^αH Val C19), 3.82 (bs, 1H, C^αHOH C11), 2.57–2.83 (m, 2H, C^αH₂ C13), 1.93–2.03 (m, 1H, C^βH Val C20), 1.58–1.68 (m, 1H, C^αH Leu C4), 1.46–1.55 (m, 2H, C^βH₂ Leu C3), 1.20 (d, $^3J=6.82$ Hz, 3H, CH₃ Ala C9), 0.88 (d, $^3J=6.57$ Hz, 3H, CH₃ Leu C5, C6), 0.83 (d, $^3J=6.32$ Hz, 3H, CH₃ Leu C5, C6), 0.78 (d, $^3J=6.57$ Hz, 3H, CH₃ Val C21, C22), 0.73 ppm (d, $^3J=6.82$ Hz, 3H, CH₃ Val C21, C22); ¹³C NMR (100.62 MHz, [D₆]DMSO): $\delta=173.86$ (C1), 171.90 (C7), 170.89 (C10), 170.37 (C20), 166.43 (C25), 134.45, 131.22, 130.37, 128.24, 127.48, 121.00 (C14–C17, C24–C27), 70.91 (C11), 58.66 (C19), 52.76 (C12), 50.20 (C2), 47.48 (C8), 39.74 (C3), 36.73 (C13), 30.19 (C20), 24.22 (C4), 22.91, 21.22 (C5, C6), 19.39 (C9), 19.13, 18.34 ppm (C21, C22); ESIMS *m/z* (*M*(norstatine)): calcd for C₃₁H₄₃N₅O₇: 597.32, found 598.4 [*M*+H]⁺.

Determination of inhibition constants toward plasmepsin II:

Plasmepsin II activity assays were performed in 96-well microtiter plates with a Tecan Spectra Fluor spectrometer at excitation wavelength 360 nm and emission wavelength 465 nm. Hemoglobin labeled with the fluorogen 7-amino-4-methylcoumarin-3-acetic acid (AMCA) was used as substrate. For IC₅₀ determinations, inhibitors were allowed to fully equilibrate with enzyme at 37 °C for 5 min. The final substrate concentration was 2.6 μM. The plasmepsin II concentration, measured by UV/Vis, was 260 nM in an acetate/formate buffer (0.06 M, pH 4.65). DMSO (2.5%) was used to guarantee complete dissolution of the inhibitors. IC₅₀ values were taken from plots of *V_i/V₀* as a function of inhibitor concentration, for which *V_i* and *V₀* are the initial rates of reaction in presence and absence of the inhibitor, respectively. Substrate hydrolysis was recorded as an increase in fluorescence intensity over a period of 3 min, during which the intensity increased linearly with time.

Determination of inhibition constants toward cathepsin D:

Cathepsin D activity assays were essentially performed as described for plasmepsin II. The pH value of the buffer, however, was changed to 3.65 and the cathepsin D concentration was 380 nM. Mature two-chain-form human cathepsin D was used. It was purified from extracts of human placental lysosomes by pepstatin affinity and cation-exchange chromatography as described previously.^[43]

Determination of inhibition constants toward HIV protease:

IC₅₀ values were taken from plots of *V_i/V₀* as a function of inhibitor concentration, for which *V_i* and *V₀* are the catalytic rates in presence and absence of the inhibitor, respectively. The fluorogenic substrate Abz-Thr-Ile-*para*-nitrophenylalanine-Phe-Gln-Arg-NH₂ was purchased from Bachem. The total enzyme concentration was 40 nM, and the substrate concentration was 20 μM. Recombinant HIV-1 protease was expressed from *Escherichia coli* and purified as previously described.^[41] Enzymatic assays were performed in 402.2 μL assay buffer (100 mM MES, 300 mM KCl, 5 mM EDTA, 1 mg mL⁻¹ BSA, pH 5.5) by adding substrate dissolved in 8.4 μL DMSO; distinct inhibitor concentrations were dissolved in 8.4 μL DMSO, and 1 μL HIV-1 protease was added to give a final volume of 420 μL (final DMSO concentration 4%). The hydrolysis of the substrate was recorded as an increase in fluorescence intensity (excitation wavelength 337 nm, emission wavelength 410 nm) over a period of 10 min, during which the rate increased linearly with time.^[49]

Virtual screening to select optimal occupancy of the S1 pocket of plasmepsin II:

Docking studies were performed with the docking program FlexX (version 1.13).^[50] As starting geometry, the crystal structure of plasmepsin II with bound EH-58 (PDB code: 1LF3) was used. Based on the coordinates of EH-58, the core structure of

the norstatine inhibitor was constructed with the P1 site unoccupied. A dataset of 500 unnatural amino acids was compiled from either the Sigma–Aldrich catalogue or the ACD. Subsequently, these residues were docked by using the *mapref* option in FlexX into the complex structure of plasmepsin II. The corresponding peptide backbone portion was considered as base fragment in *mapref*. During placement, the FlexX scoring function was applied for the final selection of the best-scored docking solutions; in addition, DrugScore was consulted.^[51]

Molecular dynamics simulation: The MD simulation and all setup steps were performed with the Amber 8.0 suite of programs,^[52] using the Amber 1999 force field. The plasmepsin structure with PDB code 1LEE was used as the starting point. The ligand and all crystallographic water molecules were removed, and hydrogen atoms were added with PROTONATE. After estimating protonation states of all histidines and of the two catalytic aspartates (Asp34 and Asp214) at pH 5 with Poisson–Boltzmann pK_a calculations, histidine groups were set to the protonated form, and the two catalytic aspartates were set to the deprotonated form. The protein was initially subjected to 200 steps of minimization with a generalized Born solvation model. Subsequently, the system was solvated in a box of ≈10300 TIP3P water molecules,^[53] and sodium ions were added to ensure neutrality. After 200 steps of minimization of the solvated system, the MD simulation was started by heating the solvent to 300 K over a period of 20 ps and cooling to 100 K over 5 ps, keeping the protein fixed. Then the entire system was brought to 300 K over a period of 25 ps, and the simulation was continued for 1 ns under NPT conditions using a time step of 2 fs and PME^[54] for evaluating the electrostatic interactions. Energy data were saved every 20 fs, and protein coordinates were saved every 0.5 ps. CARNAL was used for further analysis of the trajectory and VMD 1.8.2 was used for visualization.^[55]

Representative ¹H NMR spectra of compounds **6aa**, **6ab**, **10qa**; and **10qb** are provided in the Supporting Information.

Acknowledgements

The authors thank the DFG for funding this project under the grant Ra895-2 (“Linker reagents for the synthesis of protease inhibitor libraries”) and Kl1204-5 (“De novo design of enzyme inhibitors of plasmepsin”). Further financial support is acknowledged from Boehringer Ingelheim Pharma, Biberach, Germany, and from Merck Biosciences, L aufelfingen, Switzerland. The help of Paul Czodrowski and Alexander Hillebrecht (University of Marburg) in the computer simulations and of Graeme Nicholson (University of T ubingen) in chiral gas chromatography is gratefully acknowledged. We also thank MDL (San Leandro, CA, USA) for making the ACD compound library available to us.

Keywords: combinatorial chemistry · inhibitors · molecular dynamics · peptidomimetics · solid-phase synthesis

- [1] D. Leung, G. Abbenante, D. P. Fairlie, *J. Med. Chem.* **2000**, *43*, 305–341.
- [2] R. E. Babine, S. L. Bender, *Chem. Rev.* **1997**, *97*, 1359–1472.
- [3] J. B. Cooper, *Curr. Drug Targets* **2002**, *3*, 155–173.
- [4] O. B. Wallace, D. W. Smith, M. S. Deshpande, C. Polson, K. M. Felsenstein, *Bioorg. Med. Chem. Lett.* **2003**, *13*, 1203–1206.
- [5] D. Shuto, S. Kasai, T. Kimura, P. Liu, K. Hidaka, T. Hamada, S. Shibakawa, Y. Hayashi, C. Hattori, B. Szabo, S. Ishiura, Y. Kiso, *Bioorg. Med. Chem. Lett.* **2003**, *13*, 4273–4276.

- [6] T. Mimoto, N. Hattori, H. Takaku, S. Kisanuki, T. Fukazawa, K. Terashima, R. Kato, S. Nojima, S. Misawa, T. Ueno, J. Imai, H. Enomoto, S. Tanaka, H. Sakikawa, M. Shintani, H. Hayashi, Y. Kiso, *Chem. Pharm. Bull.* **2000**, *48*, 1310–1326.
- [7] T. S. Haque, A. G. Skillman, C. E. Lee, H. Habashita, I. Y. Gluzman, T. J. A. Ewing, D. E. Goldberg, I. D. Kuntz, J. A. Ellman, *J. Med. Chem.* **1999**, *42*, 1428–1440.
- [8] A. Lee, L. Huang, J. A. Ellman, *J. Am. Chem. Soc.* **1999**, *121*, 9907–9914.
- [9] D. Nöteberg, E. Hamelink, J. Hulten, M. Wahlgren, L. Vrang, B. Samuelsson, A. Hallberg, *J. Med. Chem.* **2003**, *46*, 734–746.
- [10] C. E. Lee, E. K. Kick, J. A. Ellman, *J. Am. Chem. Soc.* **1998**, *120*, 9735–9747.
- [11] E. Takashiro, I. Hayakawa, T. Nitta, A. Kasuya, S. Miyamoto, Y. Ozawa, R. Yagi, I. Yamamoto, T. Shibayama, A. Nakagawa, Y. Yabe, *Bioorg. Med. Chem.* **1999**, *7*, 2063–2072.
- [12] R. Nishizawa, T. Saino, T. Takita, H. Suda, T. Aoyagi, H. Umezawa, *J. Med. Chem.* **1977**, *20*, 510–515.
- [13] K. Iizuka, T. Kamijo, H. Harada, K. Akahane, T. Kubota, Y. Etoh, A. Shimaoaka, A. Tsubaki, M. Murakami, T. Yamaguchi, A. Iyobe, H. Umeyama, Y. Kiso, *Chem. Pharm. Bull.* **1990**, *38*, 2487–2493.
- [14] K. Iizuka, T. Kamijo, H. Harada, K. Akahane, T. Kubota, H. Umeyama, T. Ishida, Y. Kiso, *J. Med. Chem.* **1990**, *33*, 2707–2714.
- [15] M. M. G. M. Thunnissen, P. Nordlund, J. Z. Haeggström, *Nat. Struct. Biol.* **2001**, *8*, 131–135.
- [16] W. Yuan, B. Munoz, C. H. Wong, J. Z. Haeggström, A. Wetterholm, B. Samuelsson, *J. Med. Chem.* **1993**, *36*, 211–220.
- [17] N. P. Peet, J. P. Burkhart, M. R. Angelastro, E. L. Giroux, S. Mehdi, P. Bey, M. Kolb, B. Neises, D. Schirlin, *J. Med. Chem.* **1990**, *33*, 394–407.
- [18] H. Harada, A. Tsubaki, T. Kamijo, K. Iizuka, Y. Kiso, *Chem. Pharm. Bull.* **1989**, *37*, 2570–2572.
- [19] L. Banfi, G. Guanti, R. Riva, A. Basso, E. Calcagno, *Tetrahedron Lett.* **2002**, *43*, 4067–4069.
- [20] L. Banfi, A. Basso, G. Guanti, R. Riva, *Mol. Diversity* **2003**, *6*, 227–235.
- [21] A. Basso, L. Banfi, R. Riva, P. Piaggio, G. Guanti, *Tetrahedron Lett.* **2003**, *44*, 2367–2370.
- [22] J. E. Semple, T. D. Owens, K. Nguyen, O. E. Levy, *Org. Lett.* **2000**, *2*, 2769–2772.
- [23] R. Fernández, J. M. Lassaletta, *Synlett* **2000**, 1228–1240.
- [24] D. Enders, M. Bolkenius, J. Vázquez, J. M. Lassaletta, R. Fernández, *J. Prakt. Chem.* **1998**, *340*, 281–285.
- [25] S. Kourtal, J. Paris, *Lett. Pept. Sci.* **1996**, *3*, 73–78.
- [26] G. Veerasha, A. Datta, *Tetrahedron Lett.* **1997**, *38*, 5223–5224.
- [27] J. P. Burkhart, N. P. Peet, P. Bey, *Tetrahedron Lett.* **1990**, *31*, 1385–1388.
- [28] S. Hormuth, H. U. Reissig, D. Dorsch, *Liebigs Ann. Chem.* **1994**, 121–127.
- [29] J. Deng, Y. Hamada, T. Shioiri, S. Matsunaga, N. Fusetani, *Angew. Chem.* **1994**, *106*, 1811–1813; *Angew. Chem. Int. Ed. Engl.* **1994**, *33*, 1729–1731.
- [30] S. Weik, J. Rademann, *Angew. Chem.* **2003**, *115*, 2595–2598; *Angew. Chem. Int. Ed.* **2003**, *42*, 2491–2494.
- [31] H. H. Wasserman, K. Lee, M. D. Xia, *Tetrahedron Lett.* **2000**, *41*, 2511–2514.
- [32] R. Hua, H. Takeda, Y. Abe, M. Tanaka, *J. Org. Chem.* **2004**, *69*, 974–976.
- [33] M. Meldal, A. Papanikos, *J. Comb. Chem.* **2004**, *6*, 181–195.
- [34] C. B. Reese, R. C. Titmas, L. Yau, *Tetrahedron Lett.* **1978**, *19*, 2727–2730.
- [35] B. Blankemeyer-Menge, M. Nimtz, R. Frank, *Tetrahedron Lett.* **1990**, *31*, 1701–1704.
- [36] H. H. Wasserman, M. D. Xia, A. K. Petersen, M. R. Jorgensen, E. A. Curtis, *Tetrahedron Lett.* **1999**, *40*, 6163–6166.
- [37] A. J. Harvey, A. D. Abell, *Tetrahedron* **2000**, *56*, 9763–9771.
- [38] O. A. Asojo, S. V. Gulnik, E. Afonina, B. Yu, J. A. Ellman, T. S. Haque, A. M. Silva, *J. Mol. Biol.* **2003**, *327*, 173–181.
- [39] A. M. Silva, A. Y. Lee, S. V. Gulnik, P. Majer, J. Collins, T. N. Bhat, P. J. Collins, R. E. Cachau, K. E. Luker, I. Y. Gluzman, S. E. Francis, A. Oksman, D. E. Goldberg, J. W. Erickson, *Proc. Natl. Acad. Sci. USA* **1996**, *93*, 10034–10039.
- [40] TMSE ester **61** (Boc protected) was purified by HPLC because of lower purity ($\approx 40\%$, sensitivity to oxidation).
- [41] A. Taylor, D. P. Brown, S. Kadam, M. Maus, W. E. Kohlbrenner, D. Weigl, M. C. Turon, L. Katz, *Appl. Microbiol. Biotechnol.* **1992**, *37*, 205–210.
- [42] J. Hill, L. Tyas, L. H. Phylip, J. Kay, B. M. Dunn, C. Berry, *FEBS Lett.* **1994**, *352*, 155–158.
- [43] A. Hasilik, E. F. Neufeld, *J. Biol. Chem.* **1980**, *255*, 4937–4945.
- [44] L. Prade, A. F. Jones, C. Boss, S. Richard-Bildstein, S. Meyer, C. Binkert, D. Bur, *J. Biol. Chem.* **2005**, *280*, 23837–23843.
- [45] P.-O. Johansson, J. Lindberg, M. J. Blackman, I. Kvarnström, L. Vrang, H. Hamelink, A. Hallberg, Å. Rosenquist, B. Samuelsson, *J. Med. Chem.* **2005**, *48*, 4400–4409.
- [46] W. Adam, Y.-Y. Chan, D. Cremer, J. Gauss, D. Scheutzow, M. Schindler, *J. Org. Chem.* **1987**, *52*, 2800–2803.
- [47] W. Adam, L. Hadjiarapoglou, A. Smerz, *Chem. Ber.* **1991**, *124*, 227–232.
- [48] S. Narasimhan, R. Balakumar, *Aldrichimica Acta* **1998**, *31*, 19–26.
- [49] M. V. Toth, G. R. Marshall, *Int. J. Pept. Protein Res.* **1990**, *36*, 544–550.
- [50] M. Rarey, B. Kramer, T. Lengauer, G. Klebe, *J. Mol. Biol.* **1996**, *261*, 470–489.
- [51] H. Gohlke, M. Hendlich, G. Klebe, *J. Mol. Biol.* **2000**, *295*, 337.
- [52] D. A. Case, T. A. Darden, T. E. Cheatham, III, C. L. Simmerling, J. Wang, R. E. Duke, R. Luo, K. M. Merz, B. Wang, D. A. Pearlman, M. Crowley, S. Brozell, V. Tsui, H. Gohlke, J. Mongan, V. Hornak, G. Cui, P. Beroza, C. Schafmeister, J. W. Caldwell, W. S. Ross, P. A. Kollman, (2004), AMBER 8, University of California, San Francisco.
- [53] W. L. Jorgensen, J. Chandrasekhar, J. D. Madura, R. W. Impey, M. L. Klein, *J. Chem. Phys.* **1983**, *79*, 926–935.
- [54] T. Darden, D. York, L. Pedersen, *J. Chem. Phys.* **1993**, *98*, 10089–10092.
- [55] W. Humphrey, A. Dalke, K. Schulten, *J. Mol. Graphics* **1996**, *14*, 33–38.
- [56] K. A. Scheidt, H. Chen, B. C. Follows, S. R. Chemler, D. S. Coffey, W. R. Roush, *J. Org. Chem.* **1998**, *63*, 6436–6437.

Received: August 17, 2005

Published online on March 3, 2006